Design of a Robust Voltage Controller for a Buck-Boost Converter Using μ-Synthesis

Simone Buso, *Member, IEEE*

***Abstract*— This paper proposes the structured singular value (μ) approach to the problem of designing an output voltage regulator for a Buck-Boost converter with current-mode control. This approach allows a quantitative description of the effects of reactive components' tolerances and operating point variations, which strongly affect the converter dynamics. At first, a suitable linear converter model is derived, whose parameter variations are described in terms of perturbations of the linear fractional transformation (LFT) class. Then, μ-analysis is used to evaluate the robustness of a conventional PI voltage regulator with respect to the modeled perturbations. Finally, the approximate μ-synthesis procedure known as D-K iteration is used to design a robustly performing regulator. Simulation results are presented, describing the small and large signal behavior of a reduced order approximation of the μ-synthesized controller.**

***Index Terms*— DC-DC power conversion, H-infinity control, H-infinity optimization, robustness, uncertain systems.**

I. Introduction

DC-DC converters represent a challenging field for sophisticated control techniques' application due to their intrinsic nature of nonlinear, time-variant systems. The use of averaging or sampling techniques, followed by linearization and small-signal analysis allows the derivation of linear time-invariant dynamic models for any converter topology, but these are normally dependent on the converter's operating point. In other words, the parameters of any transfer function or state space matrix describing a dc-dc converter may vary depending on its output voltage, input voltage or load current. Nonlinear control techniques can be applied to optimize the converter large signal behavior and can provide very good results [1], [2]. The present paper, instead, proposes the use of robust control techniques to derive a controller for a dc-dc converter which is able to cope with the parameter variations in the converter's transfer function. In particular, this paper proposes the structured singular value (μ) approach [3], [4] to the design of a robust output voltage regulator for a Buck-Boost converter with current-mode control.

The paper is divided into two main sections: a modeling section, where the necessary μ-analysis set-up is developed, and a test section, where this set-up is applied. Therefore, at first, a suitable linear model for the converter is derived and the parameter variation ranges are identified. Then, an open-loop interconnection describing the plant and the parameter variations in terms of input multiplicative perturbations is built. Finally, this interconnection is augmented to allow the inclusion of a performance specification (accurate tracking of output voltage reference signal) and put into the standard linear fractional transformation (LFT) form. This gives the possibility to consider structured perturbations and theoretically allows to get to a less conservative controller design as compared to standard H_∞ synthesis [5], [6]. Moreover, once the problem is formulated in terms of LFT's it is possible to check the robust stability and robust performance conditions through the proper μ-tests. This is done in the following section, at first for a conventional PI voltage regulator. This controller represents, in fact, the standard solution for this problem and, through a worst case procedure, can be designed so as to guarantee the closed-loop stability in presence of the considered parameter variations. Nevertheless, the quality of its performance cannot be directly controlled. This can be evidenced by the application of μ-analysis to the closed-loop plant which, in fact, confirms the robustness of the stability, but also shows that the robust performance condition is not satisfied. This implies that reference voltage tracking may not be maintained for all possible parameter variations, and overshoots or lightly damped oscillations may appear in the closed-loop step response.

An effective optimization of the voltage regulator is then performed by the approximate μ-synthesis procedure known as D-K iteration, which leads to a new controller satisfying both robust stability and robust performance conditions. As usual, with this approach, the controller order turns out to be quite high making its implementation impractical. A reduced-order controller is therefore derived, which is simple enough to be practically implemented and maintains almost the same performance as the unreduced controller. Simulation results are finally given to validate both small-signal and large-signal properties of the new controller compared to the conventional solution.

II. Buck-Boost Converter Modeling

Converter Description

The circuit schematic of a Buck-Boost converter with current-mode control is shown in Fig. 1.

The Buck-Boost converter is a typical dc-dc switching converter normally used as a power supply in a wide variety of applications. Though the output voltage is what has to be regulated, it is standard practice to implement an inner current control loop, essentially to provide current limiting

Manuscript received August 8, 1997; revised April 7, 1998. Recommended by Associate Editor, G. C. Verghese.

The author is with the Department of Electronics and Informatics, University of Padova, 35131 Padova, Italy.

Publisher Item Identifier S 1063-6536(99)01614-0.

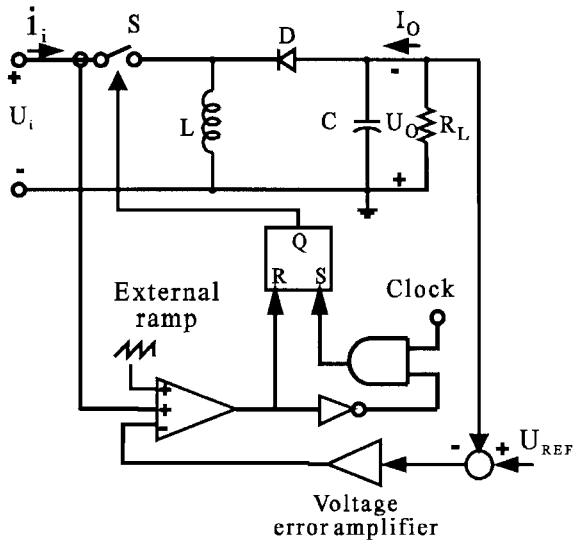

Fig. 1. Buck-Boost converter with current mode control.

TABLE I
CHOSEN CONVERTER'S PARAMETERS AND CONSIDERED VARIATION RANGES

U_i	24V ± 20%
U_O	60V
R_L	6Ω → 80Ω
L	100μH ± 20%
C	470μF ± 50%
f_{SW}	50kHz

and switch protection. In this case a peak-current-control loop is adopted [7], [8]. The chosen converter's parameters and the considered variation ranges are given in Table I. The output capacitor equivalent series resistance (ESR) is neglected in the analysis for the sake of simplicity; however, the large signal, time domain simulations, that will be presented in Section VI, have been performed both with and without the ESR in the converter's model. In this particular case, no visible effect on the converter's dynamic behavior was revealed, at least for ESR values up to 200 mΩ.

The small-signal transfer function from current reference to output voltage, that is including the current control loop, which is derived in [7] and [8], is given by (1)

$$\frac{du_0}{di_r} = R_L \cdot \frac{U_i}{U_i + 2 \cdot U_0} \cdot \frac{1 - \dfrac{s \cdot L}{R_L} \cdot \dfrac{U_0}{U_i} \cdot \dfrac{U_i + U_0}{U_0}}{1 + s \cdot C \cdot R_L \cdot \dfrac{U_i + U_0}{U_i + 2 \cdot U_0}} \quad (1)$$

the accuracy of this model has been proved [7], [8] to be very good, at least in the frequency range of interest for this application, whose upper limit can be set to about 10÷15 kHz below half the switching frequency (25 kHz). As shown, it is strongly dependent on the converter operating point and also nonminimum phase. The transfer function (1) can be rewritten

TABLE II
SELECTED VALUES

g_{0n}	8.41
τ_{zn}	1.734e-5
τ_{pn}	1.38e-2

as in (2)

$$G(s) = g_0 \cdot \frac{1 - s \cdot \tau_z}{1 + s \cdot \tau_p} = g_0 \cdot \hat{G}(s). \quad (2)$$

The values of the three transfer function parameters g_0, t_z, t_p can vary depending on the variation of the converter's physical parameters in the previously defined ranges, so that (2) actually defines a family of plants.

Perturbations Model

The effects of the parameter variations in (2) can be described by applying some kind of perturbing action to a given nominal plant. The nominal plant is chosen by selecting particular values of the transfer function parameters. The selected values are given in Table II.

Together with the adopted perturbation structure and the chosen weighting functions they define a simple model representing the effects of parameter variations in the plant, as is explained in the following.

Fig. 2 shows the open-loop interconnection of linear systems describing the plant and the adopted perturbation strategy. As can be seen, it consists of two independent input-multiplicative perturbing actions on the transfer function dc gain g_{0n} and dynamic block $\hat{G}_n(s)$. In order to describe the effects of input multiplicative perturbations, a simpler situation is considered in Fig. 3, where an elementary input multiplicative perturbation is applied to a generic plant $P(s)$. In this case, the resulting transfer function $\tilde{P}P(s)$ between u and y, which represents the perturbed plant, is given by

$$\tilde{P}(s) = [1 + \Delta(s) \cdot W(s)] \cdot P(s) \quad (3)$$

where $\Delta(s)$ is the perturbing element, that is a variable, unity-norm linear system and $W(s)$ is a weighting function whose magnitude, at every frequency, can be interpreted as the maximum relative uncertainty on the magnitude of $P(s)$ [3], [4], [9]. In the considered control design, as is shown in Fig. 2, two of these perturbation structures are cascaded to achieve an higher flexibility in the uncertainty representation. The resulting plant $\tilde{G}(s)$ has three inputs and three outputs: u is the reference current input; y_0 is the output voltage; w and z are auxiliary bidimensional input and output vectors that will be used in the following LFT structure definition.

The selection of the perturbation weighting functions is the most important aspect in the formulation of a robust control problem. The quality of the final solution, in fact, strictly depends on how good the uncertainties' representation is. Too coarse models can lead to very conservative, poor performing controllers; too sophisticated models increase the overall problem's complexity, often causing the numerical solution to

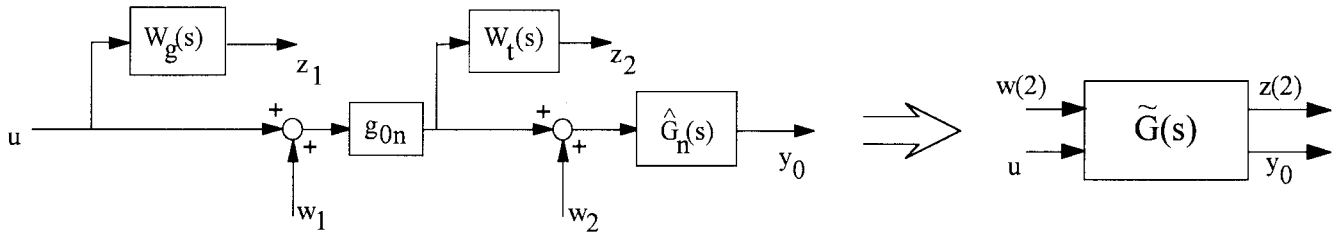

Fig. 2. Open-loop interconnection with perturbation inputs ($w+_1$ and w_2) and outputs (z_1 and z_2)—Resulting plant $\bar{G}(s)$.

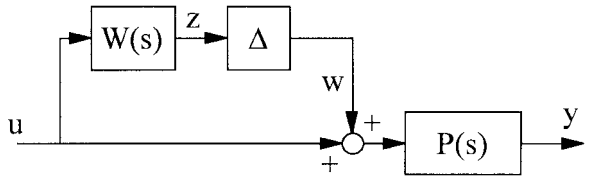

Fig. 3. Multiplicative perturbation structure.

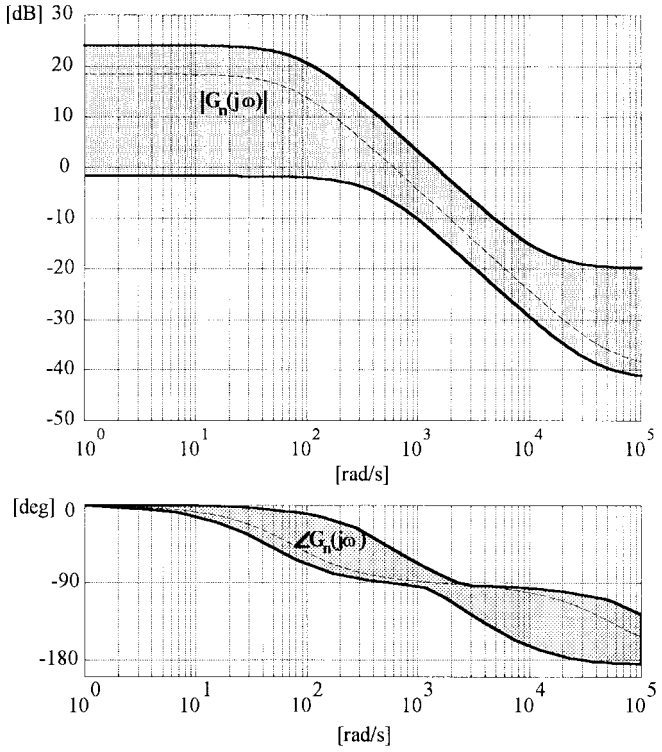

Fig. 4. Effects of the parameters' variations on $|G(j\omega)|$ and $\angle G(j\omega)$.

be ill-conditioned. Therefore, the design is constrained by the necessity of replicating, as close as possible, the global effect of the parameter variations on the nominal plant's magnitude, while keeping the model complexity as low as possible.

Fig. 4, which can be simply attained, in this particular case, by plotting the magnitude and phase of the transfer function given by (1) for a sufficiently large set of randomly selected values of the varying parameters, shows how the parameter variations affect $G(j\omega)$. Each transfer function in the set defined by (2) has magnitude and phase lying inside the shaded areas. In particular, the magnitude and phase of the nominal plant $G_n(j\omega)$ are shown (dashed line).

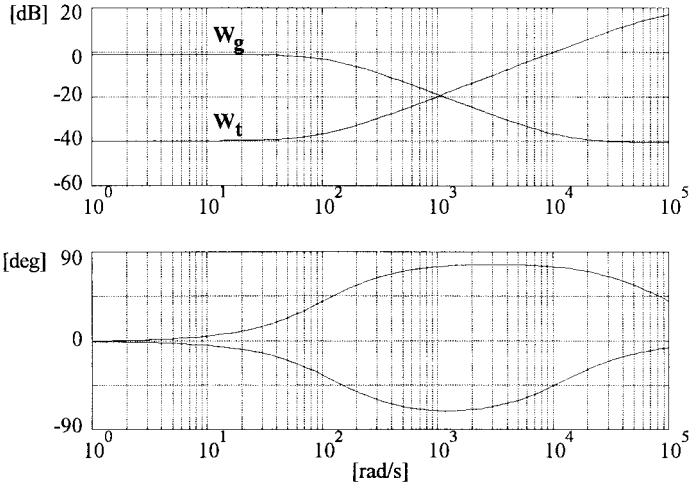

Fig. 5. Bode diagrams of perturbation weights.

The adopted weighting functions $W_g(s)$ and $W_t(s)$ are given by (4); their Bode diagrmas are shown in Fig. 5

$$W_g(s)=0.9\cdot\frac{1+s\cdot 8\cdot 10^{-5}}{1+s\cdot 8\cdot 10^{-3}},\quad W_t(s)=0.01\cdot\frac{1+s\cdot 1\cdot 10^{-2}}{1+s\cdot 1\cdot 10^{-5}}. \tag{4}$$

The open-loop interconnection shown in Fig. 2, with the indicated weighting functions and nominal plant is a simple way to model the uncertainty described by Fig. 4. In particular, the combined effect of $W_g(s)$ and $W_t(s)$ introduces a 90% uncertainty in the plant at low frequency, which accounts for the difference between the selected nominal gain g_{0n} and its maximum possible value; this uncertainty level, by a suitable choice of the function poles and zeros, with respect to the positions of the pole and the zero in the nominal plant, is then increased in the high-frequency range to reproduce the increasing difference between the nominal plant magnitude and the upper limit of the uncertainty area. The choice of the nominal plant's parameters is therefore connected to the weighting functions' design in a rather involved way, which requires a trial and error design procedure. The main drawback of this approach is its inherent conservativeness, since only the outcoming maximum magnitude of the perturbed plant can be shaped along frequency. Due to the uncontrolled variability of the phase of the total applied perturbation a much larger set of plants is generated compared to what is strictly needed to represent the effect of the physical parameter variations. On the other hand, the attained model is simple and the results, as is described in the following, are satisfactory, allowing the

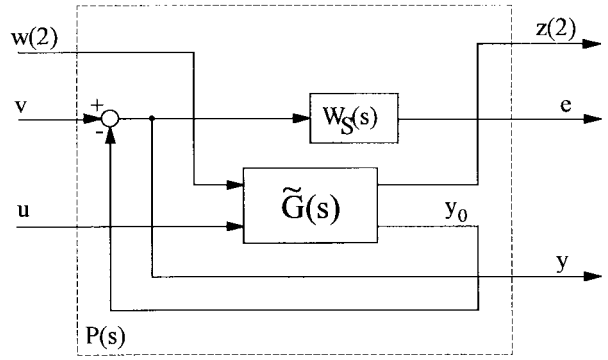

Fig. 6. Augmented plant $P(s)$.

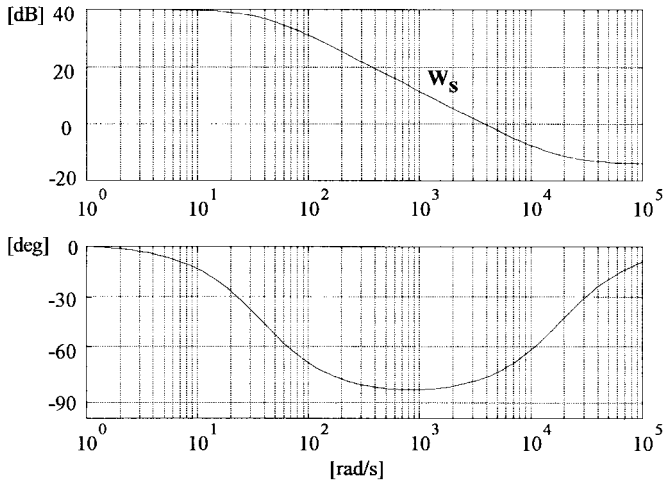

Fig. 7. Bode diagram of the performance weight W_S.

synthesis of a robust controller of reasonable complexity and effectiveness.

Performance Specification

To complete the problem's set up, it is necessary to define the performance specification for the closed-loop plant. A suitable choice for this kind of application is to ask for an accurate tracking of the output voltage reference signal. This can be done by augmenting the model so as to introduce the input and output channels necessary to formulate this performance specification. The resulting interconnection is shown in Fig. 6 and is called $P(s)$.

Referring to Fig. 6, once the control loop is closed by inserting a controller between output y and input u, the transfer function between input v, which is the reference voltage input, and output e, which is the tracking error filtered by $W_S(s)$, is the product of the closed-loop sensitivity of the plant $S(s)$ and of the performance weight $W_S(s)$. If condition (5) holds then, as in any standard H_∞ control problem [5], the sensitivity transfer function is shaped in frequency according the profile specified by $1/W_S(s)$

$$||W_s S||_\infty < 1. \tag{5}$$

Typically, the sensitivity needs to be kept low at low frequency, so as to allow accurate tracking (e.g., within 1%)

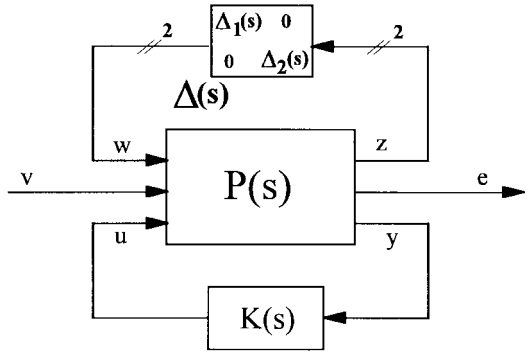

Fig. 8. Complete LFT structure.

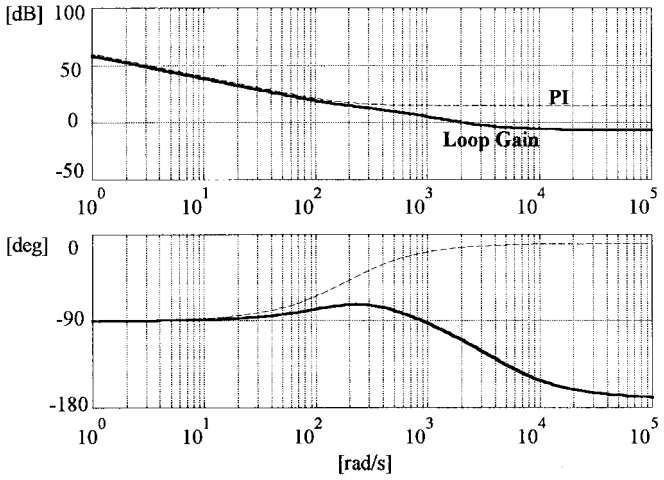

Fig. 9. PI regulator and worst-case-loop gain.

of the reference signal, which is constant in steady-state. Since the sensitivity also tends to unity at high frequency, the weight $W_S(s)$ must be low-pass. The expression for the chosen $W_S(s)$ is given by (6), while its Bode diagram is shown in Fig. 7

$$W_s(s) = 100 \cdot \frac{1 + s \cdot 5.3 \cdot 10^{-5}}{1 + s \cdot 2.6 \cdot 10^{-2}}. \tag{6}$$

It is worth noting that the positions of the pole and zero in the transfer function W_S are relevant in the design under different points of view. On the one hand, keeping W_S's crossover frequency high tends to increase the closed-loop plant bandwidth and so to accelerate the system dynamic response; on the other hand, increasing the required dynamic performance level makes it more difficult to achieve the needed robustness. As a consequence, the choice of the pole and zero positions involves a tradeoff. In this case, the selected pole and zero positions guarantee a satisfactory performance level, which can be maintained in presence of the considered perturbations; a more demanding W_S's profile may not be compatible with the required robustness.

LFT Structure

The complete weighted interconnection in the LFT form, which represents the standard setup for μ-analysis and synthesis, including the perturbing matrix $\Delta(s)$ and the controller $K(s)$, is shown in Fig. 8. The perturbing matrix $\Delta(s)$ is a 2×2

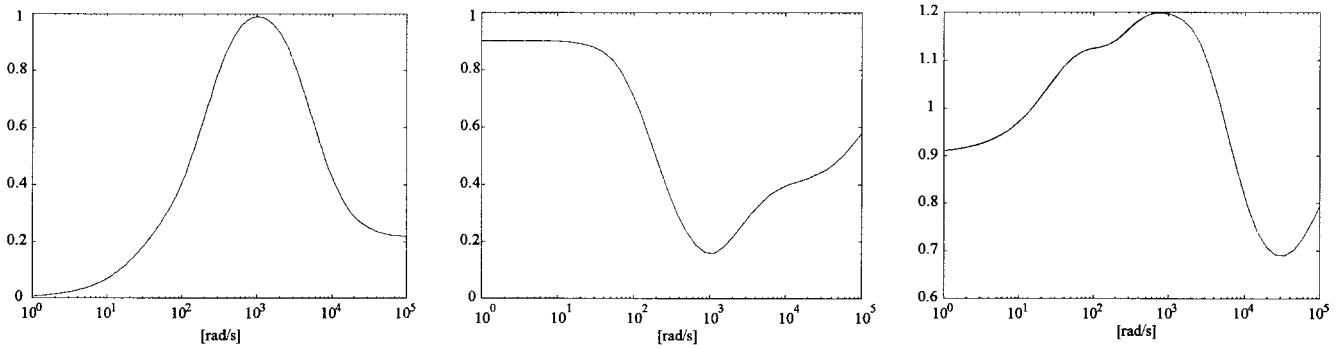

(a) (b) (c)

Fig. 10. (a) Magnitude of norminal weighted sensitivity. (b) μ for robust stability. (c) μ for robust performance.

diagonal matrix whose elements are two complex scalars, each having unity maximum magnitude and acting as the perturbing element Δ of Fig. 3. This matrix is inserted between output z_1, z_2 and inputs w_1, w_2 of Fig. 3, thus closing the perturbing loop. The controller $K(s)$ can be any stabilizing controller for plant $P(s)$. Also the performance input and output v and e are available for robust performance tests.

III. PI Regulator Design

Taking into account the parameter variations indicated by Table I, it is possible to design a conventional PI regulator so as to ensure, in the worst operating conditions, a suitable crossover frequency and phase margin for the open-loop gain. It is possible to see that the worst conditions take place when input voltage and load resistor are minimum while inductor and capacitor values are maximum, because in this case the gain and phase of the plant are minimum in the crossover region. In these conditions a PI regulator was designed to provide a 400 Hz crossover frequency and a 60° phase margin. Even if more sophisticated classical controllers may exhibit a better behavior, the PI regulator is often adopted in practice, thanks to its design simplicity. Indeed, it guarantees stability and, at least in nominal conditions, a satisfactory performance level for the closed-loop plant. On the other hand, as will be shown in the following, the robustness of the achievable performance is quite poor. The Bode diagrams of the regulator and open-loop gain are shown in Fig. 9.

IV. μ-Analysis of PI Regulator

The robustness properties of the PI regulator can be tested by executing the proper μ-tests for the closed-loop system of Fig. 8, once the controller $K(s)$ is substituted by the PI. The robust stability property of the controller can be tested by calculating the infinity norm (peak value over frequency) of μ with respect to the perturbing matrix Δ: if this turns out to be less than unity, the system is robustly stable [3], [4], [9].

As far as the performance is concerned, the nominal performance condition has to be checked first. This is done by evaluating the infinity norm of the closed-loop weighted sensitivity, when no perturbing action is applied, that is to say when the regulator operates on the nominal plant. As in any standard H_∞ synthesis, if this norm turns out to be less than unity, so that condition (5) holds, the regulator achieves nominal performance. This is equivalent to saying that the closed-loop sensitivity has the desired frequency profile at least in the nominal case. To test the robust performance condition, it is necessary to calculate the infinity norm of μ with respect to an augmented perturbing matrix that has to include an auxiliary, full, complex, diagonal block operating on the performance inputs and outputs. It is worth noting that, in this particular case, the needed auxiliary block is scalar. The *main-loop theorem* [3], [4], [9] then, states that the closed-loop plant achieves robust performance if and only if the norm of μ, calculated in these conditions, is less than unity. The results of these calculations are illustrated by Fig. 10 which shows that the PI controller achieves nominal performance [Fig. 10(a)] and robust stability [Fig. 10(b)], since the corresponding norms are less than one.

This result agrees with the worst case procedure followed in the PI regulator's design, which was aimed at ensuring the stability of the plant in presence of parameter variations while keeping the tracking error e as small as possible. Besides, it can also be interpreted as a validation of the adopted perturbation model, that turns out to correctly replicate the effects of parameter uncertainty.

However, it is possible to see that the PI regulator does not guarantee robust performance because the corresponding infinity norm of μ is 1.2. This means that among the modeled perturbations there is one, whose size is 1/1.2, which can cause the degradation of the closed-loop performance.

V. Application of μ-Synthesis

Using μ-synthesis, it is possible to find a controller, if one exists, that not only internally stabilizes plant P, but also minimizes the infinity norm of μ so as to get robust performance. As is shown in [3] and [9], the direct solution of this problem is not possible; nevertheless the software tools employed in the present work [9] allow an approximate solution based on the iterative procedure known as D-K iteration. After a few iterations a controller achieving the robust performance objective is found. Robust stability and robust performance μ-plots are given in Figs. 11 and 12, respectively (solid line). Both have peak values that are less

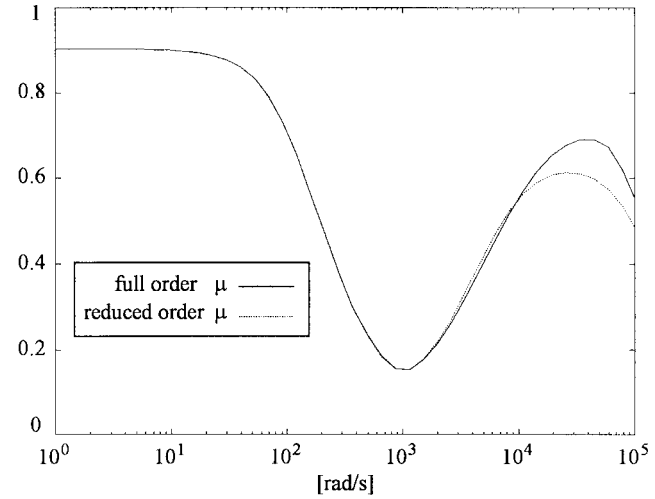

Fig. 11. Robust stability μ plot.

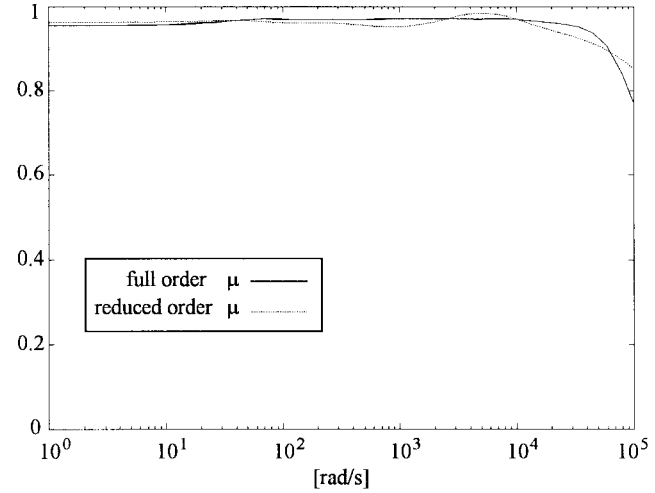

Fig. 12. Robust performance μ plot.

than unity, which implies the robustness of these properties with respect to the modeled perturbations.

The drawback of the μ-synthesized controller is that it has 16 states; therefore its practical implementation is not easily feasible. To overcome this limitation, various order-reduction techniques can be adopted [9]. In particular, using a balanced stochastic reduction algorithm [9], it is possible to find a third-order approximation of the full controller that provides a rather accurate replication of its magnitude and phase in the frequency range of interest. The results of the μ-tests for the reduced order controller are shown in Figs. 11 and 12 (dotted line). The Bode plots of the PI regulator, the full-order μ-synthesized controller and the reduced-order controller are shown in Fig. 13. Notice the similarity of the three diagrams, especially in the crossover frequency region, confirming the good properties of the PI solution which is indeed very close to the optimal one represented by the μ-synthesized controller. Still, the PI regulator does not ensure robust performance and some refinement is required to avoid performance degradation in presence of perturbations. Globally, the optimization procedure results in a limitation of the dc gain and bandwidth of the regulator.

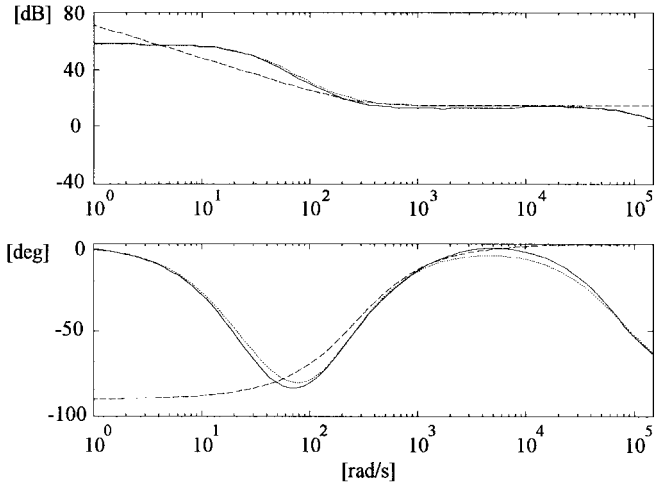

Fig. 13. Bode diagram of the three contollers: PI (dashed), full order u (solid), reduced order μ (dotted).

VI. Evaluation of Performance

The performances of PI, full-order, and reduced-order μ controllers can be verified by simulating the closed-loop step responses both in the nominal condition and in presence of perturbations. The software tools [9] employed in this work allow to determine the worst case perturbing matrix for any of the considered closed-loop plants.

For the PI controller, in particular, this is the perturbing matrix Δ whose size in terms of infinity norm is 1/1.2, which corresponds to the peak value of μ (1.2) in the frequency range of interest [Fig. 10(c)]. Applying this perturbation to all closed-loop plants, it is possible to evaluate the differences in the controllers' performance.

As shown in Fig. 14, while both the μ controllers maintain a good performance with reduced overshoot and oscillations in any condition, the performance of the PI regulator may exhibit a strong degradation. The step response in perturbed conditions, as shown in the middle (long simulation time) and bottom (short simulation time) parts of Fig. 14, is in fact characterized by high-frequency oscillations and a considerable overshoot. This further demonstrates the superior robustness of the μ controller.

Moreover, Fig. 14 shows that the reduction of the controller order from 16 to three states, which makes its implementation practical, can be attained without significantly worsening the performance. It is important to notice that these time-domain simulations are showing only the small-signal behavior of the controllers. The large signal behavior can be tested considering a more detailed simulation in which the overall converter operation, including the inner current control loop and PWM switching process, can be modeled.

The results of these simulations, which were performed by using the continuous system modeling program (CSMP), are shown in Fig. 15. As can be seen, the reduced order μ-synthesized controller exhibits a good large- signal behavior both for reference voltage (in light-load and full-load conditions) and load resistance step variations, which further confirms its practical applicability. In particular, it is possible

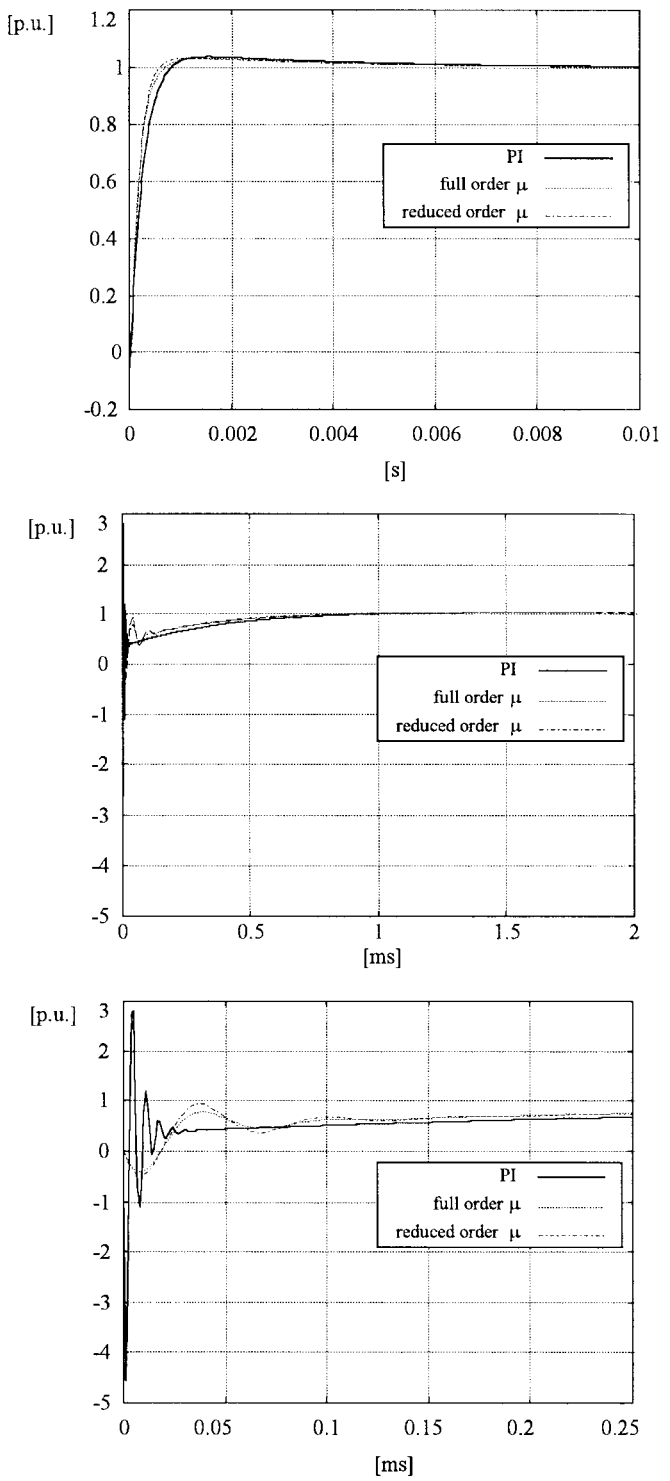

Fig. 14. Step responses of the closed-loop plant in nominal (top) and perturbed conditions (middle and bottom) for the different controllers.

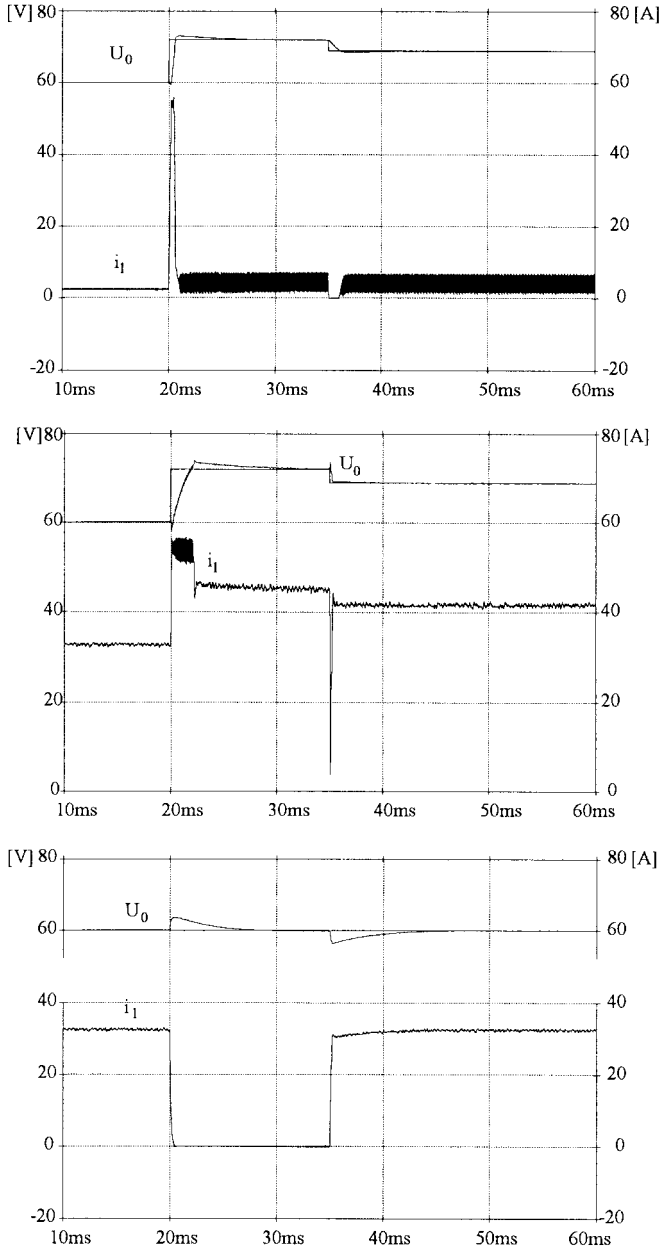

Fig. 15. Reduced-order μ-controller: effects of reference voltage step changes for light load (top) and full load (middle). Effects of load current step changes (bottom).

to notice a good speed of response, with reduced overshoot even in the presence of current-loop saturation.

VII. Conclusions

The application of μ-analysis and synthesis to the design of a robust voltage controller for a Buck-Boost converter with peak current control is presented. This represents a possible solution to the problem of large parameter variations in the converter's transfer function. The resulting μ-controller is compared to a conventional PI regulator by testing robust stability and performance of both, through the proper μ-tests. The adopted model for perturbations is also described. This turns out to be quite simple also because a resistive load is assumed throughout the analysis; more complicated models may be needed to account for nonresistive loads. Based on this model, a reduced-order controller is then derived whose practical implementation is feasible.

Finally, the performance of the reduced order μ-controller is compared by simulations to that of the PI regulator both in the small-signal and in the large-signal domain. The results demonstrate the superiority of the μ-controller and that, in

this case, robust performance can be achieved with no need for a very complicated controller structure, by modeling plant uncertainties according to the described LFT structure.

REFERENCES

[1] P. Mattavelli, L. Rossetto, G. Spiazzi, P. Tenti, "General-purpose fuzzy controller for dc-dc converters," in *Proc. IEEE Appl. Power Electron. Conf. (APEC)*, Dallas, Mar. 1995, pp. 723–730.

[2] ———, "General-purpose sliding-mode controller for dc/dc converter applications," in *Proc. IEEE Power Electron. Specialists Conf. (PESC)*, Seattle, June 1993, pp. 609–615.

[3] A. Packard and J. Doyle, "The complex structured singular value," *Automatica*, vol. 29, no. 1, pp. 71–109, 1993.

[4] A. Packard, J. Doyle, and G. Balas, "Linear, multivariable robust control with a μ perspective," *Trans. ASME*, vol. 115, June 1993, pp. 426–438.

[5] H. Kwakernaak, "Robust control and H_∞-optimization-tutorial paper," *Automatica*, vol. 29, no. 2, pp. 225–273, 1993.

[6] R. Naim, G. Weiss, and S. Ben-Yaakov, "H_∞ control of boost converters," in *APEC Conf. Proc.*, 1995, pp. 719–722.

[7] R. B. Ridley, "A new continuous-time model for current-mode control," in *Power Conversion Intell. Motion (PCIM) Conf. Proc.*, 1989, pp. 455–464.

[8] J. G. Kassakian, M. F. Schlecht, and G. C. Verghese, *Principles of Power Electronics*. Reading, MA: Addison-Wesley, 1991.

[9] G. Balas, J. Doyle, K. Glover, A. Packard, and R. Smith, "μ-analysis and synthesis toolbox," MuSyn Inc. and The Math Works Inc., 1990.

Simone Buso (M'98) was born in Padova, Italy, in 1968. He received the M.Sc. degree in electronic engineering from the University of Padova, Padova, in 1992 and the Ph.D. degree in industrial electronics from the University of Padova in 1997.

Since 1993 he has joined the Power Electronics Laboratory of the University of Padova. He is currently a Researcher of the Department of Electronics and Informatics of the University of Padova, Padova, Italy. His main research interests include dc/dc converters, digital control, and robust control of power converters.